Role of Short-Range Electrostatics in Torsional Potentials[†]

Michael G. Darley and Paul L. A. Popelier*

Manchester Interdisciplinary Biocentre (MIB), 131 Princess Street, The University of Manchester, Manchester M1 7DN, Great Britain

Received: April 15, 2008; Revised Manuscript Received: July 23, 2008

A force field needs to decide if it should contain a torsional potential or not. A helpful guide to this decision should come from a quantum mechanical energy partitioning. Here we analyze the energy profiles of eight simple molecules (ethane, hydrogen peroxide, hydrazine, methanol, acetaldehyde, formamide, acetamide and *N*-methylacetamide) subject to rotation around a torsion angle. Coulomb interaction energies between all atom pairs in a molecule are monitored during the rotation. Atoms are defined as finite electron density fragments by quantum chemical topology, a method that enables well-defined short-range interactions (1−2, 1−3 and 1−4). Energy profiles of Coulomb interaction energies mostly counteract the ab initio energy profiles. This and future work strives to settle ambiguities in current force field design.

1. Introduction

Understanding intramolecular rotation, of one or several parts of a molecule around a bond relative to the remaining part, is central to conformational chemistry. Understanding rotation around torsion angles and the concomitant energy barriers is vital to predicting the conformations of biologically systems. The backbone conformation of a polypeptide, for example, is specified by rotation along pivotal torsion angles: φ about the C_α−N bond and Ψ about the C_α−C bond. Indeed, the folding of proteins (helices, pleated sheets and turns) is defined by conformation maps or Ramachandran diagrams in terms of φ and Ψ. This illustrates the central role of rotation around bonds. Recent microwave spectroscopy studies[1] of peptide pilot systems such as formamide,[2] acetamide and *N*-methylacetamide demonstrate the unique dynamical structure of the peptide linkage system.

Ethane is often used as a model system for studying internal rotation. In 1936 Kemp and Pitzer[3] showed that the internal rotation of ethane has three minima and modeled its potential energy profile via the expression $^1/_2V_0(1 - \cos 3\omega)$. Much later (molecular mechanics) force fields adopted similar functional forms to describe rotation around a variety of bonds. However, not all force fields use torsion potentials. Nonbonded interactions between the atoms at the end of a torsion angle (the 1,4 atoms) can also describe a torsional energy profile. Still, most force fields for organic molecules do use explicit torsion potentials, with a contribution from each bonded quadruplet of atoms (ABCD) in the system.[4] Assigning separate and additive potentials to sequences of four atoms assumes that local energy profiles can be reduced to an interaction between those atoms. A lucid and reliable procedure to partition energy is thus warranted to put torsion potentials on a firm footing. That there is a need for this is substantiated by the fact that the torsion potentials of popular force fields are often the source of the differences in the energy and structures predicted by these force fields. Changes to the torsional potential can drastically affect the accuracy of the force field.[5,6] For example, setting the φ

and Ψ torsion potentials in the original AMBER-94 to zero led to much better agreement with experimental helix-coil parameters.[7]

In four-atom molecules such as hydrogen peroxide there is no need for atomic partitioning. The profile of the total molecular energy in response to a change in the central OO torsion angle must be due to all interactions between the four atoms. However, even when there are only four atoms the actual origin of the rotation barrier would be controversial according to the present literature,[8−14] which advocates or criticizes steric repulsion and hyperconjugation as possible explanations. The current paper is *not* addressing the contentious issue of the origin of rotation barriers. Instead, we focus on what we can learn from a careful and physically justifiable partitioning of energy in terms of atomic contributions for a set of pilot molecules biased toward peptides. Ultimately, decisions made in the partitioning scheme regulate the interpretation of rotation barriers. It is important that the partitioning scheme is minimal, which is not to be confused with simple. The qualifier "minimal" refers to the number and nature of the assumptions, rather than to the computational complexity or cost of the partitioning procedure. Future force fields should eliminate the necessity for ad hoc manipulation of their torsion terms as illustrated above. Narrowing the gap between a priori force field potentials and ab initio reduced density matrices, the underlying quantum reality helps or perhaps even guarantees achieving this ultimate goal. This paper focuses on well-defined short-range Coulomb interaction obtained from atomic electron density fragments.

The partitioning scheme chosen in this work is quantum chemical topology (QCT).[15,16] QCT can be used to break down the interactions within a molecule into 1−2 interactions (atoms separated by one bond), 1−3 interactions (atoms separated by 2 bonds) and 1−4 interactions (atoms separated by three bonds or more). Studying these interactions for atoms involved in torsion angles reveals the short-range electrostatics involved in torsion potentials. Molecular energy can be simultaneously partitioned into atomic contributions and into physical terms (kinetic, Coulomb, exchange). Such examination has been accomplished before[17] with QCT for five simple systems (H_2, CO, H_2O, $(HF)_2$ and $(H_2O)_2$) by distorting these systems from their equilibrium geometry and monitoring how the various

Short-Range Electrostatics in Torsional Potentials

J. Phys. Chem. A, Vol. 112, No. 50, 2008 **12955**

atomic energy contributions vary upon a change in nuclear coordinates. Although such a full energy analysis reveals all the behavior and relative importance of all the types of interaction, it is computationally expensive. In a parallel development the Oviedo group has produced a substantial number of QCT energy partitioning studies under their interacting quantum atom (IQA) approach,[18] enabling many qualitative ideas about the chemical bond being quantified.[19] The method splits the total energy into intra- and interatomic components and is applicable to quite general wave functions.[20] Here we do not perform a full energy partitioning but restrict ourselves to the atom–atom Coulomb energy for the 1–2, 1–3 and 1–4 interactions. These interactions can be computed exactly by means of a six-dimensional integration but a multipole expansion offer a faster route. The price paid for this route is possible lack of convergence, although QCT multipole moments perform[21] favorably compared to DMA[22] ones. At short-range the use of multipole moments is vital to guarantee realism and accuracy. The satisfactory convergence of QCT atomic multipole moments in the reproduction of electrostatic potentials[23] and electrostatic atom–atom interaction[24,25] was demonstrated a while ago. The convergence sphere can be expanded using continuous "Bessel moments"[26] and more dramatically by "inverse moments".[27] Exchange energy can also be successfully expanded in terms of QCT "exchange moments".[28] QCT multipole moments are also successful in the prediction of the structure of nucleic acid base pairs,[29] hydrated amino acids[30] and the dynamics of liquids.[31–33] Concerns about the efficiency and practicality of a high-rank multipolar force field were addressed in work[34] that determined which rank is necessary to have the electrostatic energy converge to the exact interaction energy within a certain error margin. More importantly, for this study, we showed that by shifting[35] the expansion sites further away from each other the 1–3 and 1–4 interactions can be expressed as a convergent multipole expansion.[36] The conceptual importance of this result is that 1–3 and 1–4 interactions, which are normally classified as "bonded" interactions, can be treated as if they were nonbonded interactions, at least in terms of Coulomb interaction.

Our work is further motivated by a study[21] of Dudek and Ponder on the energy surface of blocked alanine showing that the addition of the 1–3 interaction to the electrostatic energy substantially improves the accuracy of a force field. This is also true for the 1–2 interaction, which deserves much attention in the current study. Finally, we point out that this work must be viewed in the context of a "multipolar research program". Although biomolecular force fields are still dominated by point charges, this program is also carried forward by other groups that gauge[37–47] the impact of multipole moments on energetic, structural and dynamical calculations.

2. Background and Computational Details

2.1. Quantum Chemical Topology. Because details on the definition and practical construction of QCT atoms (or topological atoms in short) can be found elsewhere,[15,16] we only highlight the essence here. A central idea in the QCT approach is the gradient path. This is a trajectory of steepest ascent, in this case, in the electron density ρ. A multitude of gradient paths originate at infinity and terminate at a nucleus. Such a bundle of gradient paths carves out a portion of space, which is associated with a topological atom. Figure 1 illustrates the topological atoms appearing in *N*-methylacetamide generated by a novel algorithm[48] based on finite elements. Interatomic surfaces mark the atomic boundaries inside the molecule and the $\rho = 10^{-2}$ au contour surface delineate the outer boundaries. Superimposed

on this picture is the so-called molecular graph,[16] which expresses the bonding pattern. Such pictures illustrate the intuitive character of the topological features of the electron density. The superposition in Figure 1d helps in appreciating how the atoms deform upon rotation around the peptide torsion angle at the center of the molecule.

2.2. Energy Partitioning. Because a full energy partitioning will be discussed for a Hartree–Fock wave function of ethane only, some relevant background needs to be given here. It can be shown[17] that the total (restricted) Hartree–Fock energy of a molecule can be expressed as

$$E_{\text{TOT}} = \sum_{A} E_{\text{kin}}^{A} + \frac{1}{2}\sum_{A,B} E_{\text{Coul}}^{AB} + \frac{1}{4}\sum_{A,B} E_{X}^{AB} \tag{1}$$

where E_{kin}^{A} is the kinetic energy associated with the topological atom A. Topological atoms can coincide (A = B) and in this case the Coulombic energy between a topological atom and itself, E_{Coul}^{AA}, is called the *Coulomb self-energy*. When A and B do not coincide, E_{Coul}^{AB} is called the *Coulomb interaction energy*. The exchange energy is also decomposed into an *exchange self-energy* E_{X}^{AA} and an *exchange interaction energy* denoted by E_{X}^{AB} with A $\neq$ B. The total Coulomb energy between two atoms A and B is given by a six-dimensional integral:

$$E_{\text{Coul}}^{AB} = \int_{\Omega_A} d\mathbf{r}_1 \int_{\Omega_B} d\mathbf{r}_2 \frac{\rho_{\text{tot}}(\mathbf{r}_1)\,\rho_{\text{tot}}(\mathbf{r}_2)}{|\mathbf{R} + \mathbf{r}_2 - \mathbf{r}_1|} \tag{2}$$

where Ω represents the atomic volume. The denominator can be identified with the separation between electronic charge, where $\mathbf{R} = \mathbf{R}_B - \mathbf{R}_A$, and $\mathbf{R}_A$ and $\mathbf{R}_B$ represent the nuclear coordinates of atoms A and B, respectively. The total charge density, $\rho_{\text{tot}}(\mathbf{r})$, is the sum of the nuclear and electronic charge density. It is convenient to absorb the nucleus-electron interaction, E_{ne}^{AB}, and the nucleus–nucleus interaction, E_{nn}^{AB}, inside the Coulomb energy. Doing so (see eq 2), E_{Coul}^{AB} now represents the total Coulomb energy between the *charge* densities (nuclear and electronic) of two topological atoms. The exchange energy term, E_{X}^{AB} (see eq 1) can be expressed as

$$E_{X}^{AB} = -\int_{\Omega_A} d\mathbf{r}_1 \int_{\Omega_B} d\mathbf{r}_2 \sum_{ij} \frac{S_{ij}(\mathbf{r}_1)\,S_{ij}(\mathbf{r}_2)}{|\mathbf{R} + \mathbf{r}_2 - \mathbf{r}_1|} \tag{3}$$

where the overlap function S_{ij} is written in terms of two molecular orbitals ψ_i and ψ_j as

$$S_{ij}(\mathbf{r}) = 2\psi_i(\mathbf{r})\,\psi_j(\mathbf{r}) \tag{4}$$

The total self-energy, E_{self}, represents the sum of the intra-atomic energies, as defined in eq 5,

$$E_{\text{self}} = \sum_{A} E_{\text{kin}}^{A} + \frac{1}{2}\sum_{A} E_{\text{Coul}}^{AA} + \frac{1}{4}\sum_{A} E_{X}^{AA} \tag{5}$$

The total interaction energy, E_{inter}, represents the sum of the interatomic energies:

$$E_{\text{inter}} = \frac{1}{2}\sum_{A}\sum_{B \neq A} E_{\text{Coul}}^{AB} + \frac{1}{4}\sum_{A}\sum_{B \neq A} E_{X}^{AB} \tag{6}$$

At the Hartree–Fock level all energy terms are well-defined or "pure" in that the kinetic energy is "uncontaminated" and so is the exchange term. This is not true for B3LYP wave functions where the Kohn–Sham formalism applies. In Kohn–Sham density-functional theory the total electronic energy of the real, fully interacting system is expressed as

$$E_{tot} = T_0 + \int d\mathbf{r}\, \rho(\mathbf{r}) V_{nuc} + \frac{1}{2} \int \int d\mathbf{r}_1\, d\mathbf{r}_2\, \frac{\rho(\mathbf{r}_1)\, \rho(\mathbf{r}_2)}{r_{12}} + E_{XC}$$

(7)

where T_0 is the kinetic energy of an (*artificial*) *noninteracting* reference system, and the second and third term the nuclear interaction energy and the Coulomb energy, respectively. The last term, E_{XC}, defines the Kohn–Sham exchange–correlation energy. It contains all the details of two-body exchange and a kinetic-energy component. The Coulomb term is clearly "pure" and valid, being identical in both DFT and HF schemes. This term is the focus of this paper.

2.3. Torsion Energy Profiles. Eight small molecules were optimized at the B3LYP/6-311+G(2d,p) level of theory using GAUSSIAN03.[49] One torsion angle in each molecule was then chosen to be rotated and a single point calculation performed for each torsion angle. All calculations were performed without imposing symmetry constraints. The default optimization criteria do not necessarily lead to perfectly symmetric optimized end geometries. For our purposes, small deviations (e.g., 0.1° in a torsion angle) are negligible. In total eleven torsion angles were monitored, as shown in Figure 2.

For each molecule two different rotations were performed, namely rigid and relaxed. During the rigid rotation only the torsion angle was varied (in 10° steps) with all other bond angles, bond lengths and dihedrals fixed at the optimized values. During relaxed rotation all bond angles, bond lengths and dihedrals are allowed to reoptimize while the torsion angle of interest remains fixed. However, because of the 10° increments the actual minimum is sometimes stepped over. For example, in hydrogen peroxide, the minimum energy torsion angle of 115.9° is taken as 120° because this is the closest angle. The reason for the dual treatment is triggered by the literature on the origin of rotation barriers. Some explanations highlight the role played by the lengthening of the central C–C bond in ethane by 0.014 Å, as the conformation changes from staggered to eclipsed. Goodman et al.[50] state that the barrier mechanism cannot be understood in terms of rigid rotation, that is, without taking into account skeletal relaxation. This view is not shared by Song et al.[12] who claim that both rigid and relaxed rotations have the same mechanism. Although the relaxed analysis is closer to the reality of the intrinsic reaction path corresponding to a conformational change, the rigid analysis is popular and often features in force field commentaries. However, Goodman extensively commented[51] on the confusion that has resulted from the lack of a unique description of internal rotation. He warns against the "faulty description" of a rigid-rotation path and claims that even fully relaxed rotation is ambiguous. In that
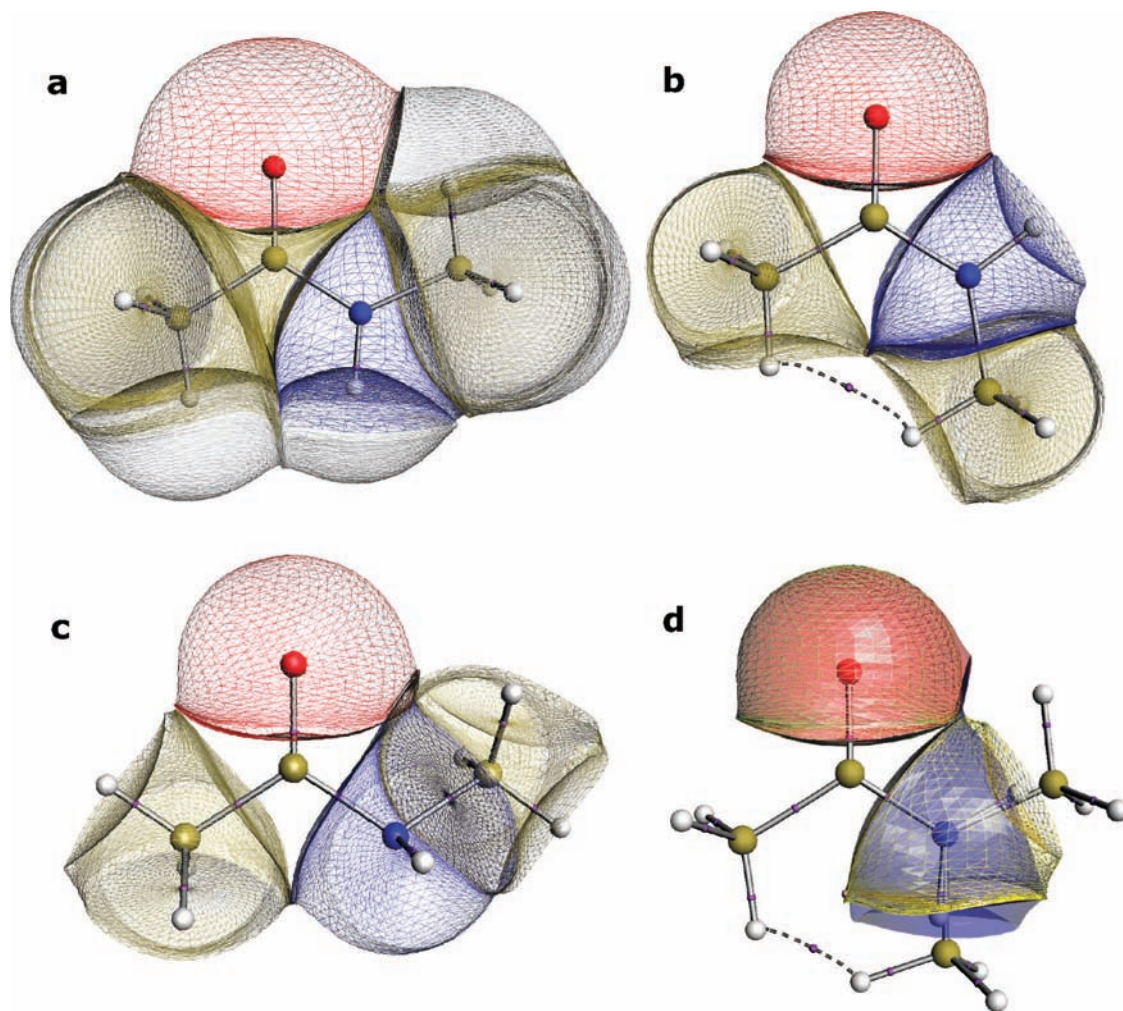

Figure 1. Finite element representation of the topological atoms in *N*-methylacetamide. Bond critical points are marked by purple spheres and atomic interaction lines are marked by solid lines. Interatomic surfaces constitute the atomic boundaries inside the complex, and the $\rho = 10^{-2}$ au contour surface denotes the outer boundaries. (a) All atoms for the optimized conformation in which the central torsion angle ω (O=C–N–H) is 180°. (b) Selection of atoms in the $\omega = 0°$ conformation where a ring critical point appears, marked by a pink sphere. (c) Selection of atoms for $\omega = 90°$. (d) Superposition of two oxygen and two nitrogen atoms, each sampled from the $\omega = 180°$ (solid) and $\omega = 0°$ (wireframe) conformations, along with the respective molecular graphs.

Short-Range Electrostatics in Torsional Potentials

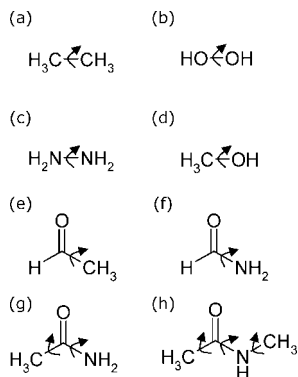*J. Phys. Chem. A, Vol. 112, No. 50, 2008* **12957**

Figure 2. Schematic representation of the eleven torsion angles varied in the set of eight molecules: (a) ethane C−C rotation, (b) hydrogen peroxide O−O rotation, (c) hydrazine N−N rotation, (d) methanol C−O rotation, (e) acetaldehyde C−C rotation, (f) formamide C−N rotation, (g) acetamide C−C and C−N rotation and (h) *N*-methylacetamide $C_{carbonyl}$−C, $C_{carbonyl}$−N and N−C_{methyl} rotation.

case the torsion angle is not fully defined. When the methyl rotation is studied, for example, the "reference" hydrogen rotation angle (HCCX), which controls the rotation, is precisely fixed. However, the other two methyl hydrogens do not necessarily undergo the same angles of rotation. We observed this in ethane where the 3-fold symmetry was broken. In ethane six CH 1−2 interaction energies coagulated in three pairs of identical energy, each displaying a different profile (but intersecting at 0° and 60° because of D_{3h} and D_{3d} symmetry, respectively). This unexpected symmetry (or lack of higher symmetry) during the torsional rotation is mirrored in the way the CH bond lengths change. Pairing can be induced between given CH bonds as a consequence of the choice of the reference torsion angle that controls the rotation. Because the choice of the reference torsion angle is arbitrary there is no point in reporting the individual CH energy profiles. However, it does make sense to report certain sums of atom−atom interaction energies. For example, the sum of the three CH energies occurring in methyl is meaningful, as well as the sum of all 1−2 interactions in a molecule. In summary, torsional rotation is not a straightforward concept, which makes it difficult to compare theory and experiment.[51] Rotation barriers are well-defined quantities, however, because they are the difference between stationary points on a full multidimensional potential energy surface. The main aim of this paper is to monitor atomically partitioned Coulomb energies during a molecular motion that is controlled by a torsion angle. In spite of the recognized ambiguity of relaxed rotation we believe that this is the best representation for our purposes, compared to rigid rotation. Because of this reason and not to overburden the paper by doubling the number of figures, we focus on the relaxed rotation, though we occasionally mention rigid rotation results.

There is one final technical remark. The relaxation of the nuclear skeleton upon torsional rotation can lead to unexpected effects. Figure S1 (Supporting Information) illustrates the example of acetamide where the energy profile has a maximum at 80° but then shows a drop in energy upon rotation to 90°. This drop in energy is due to one of the N−H bonds (N3–H5) relaxing into the O=C−N plane.

2.4. Multipole Expansion for Short-Range Interactions. The wave function files generated by the single point calculations are used by the computer program MORPHY[52,53] to calculate the multipole moments for each atom in the molecule. The moments are defined within the spherical tensor formalism,[24,54] which renders them irreducible and hence more

compact than Cartesian tensors. Multipole moments are designated by a rank *l*, which is 0 for monopole moments, 1 for dipole moments, 2 for quadrupole moments etc. The interaction between multipole moments on atom A and atom B is labeled by the interaction rank $L = l_A + l_B + 1$. To calculate the 1−2 interaction energy, an exact (six-dimensional) integration is performed, as shown in eq 2. For the 1−3 interaction energy interaction ranks up to $L = 30$ may need to be evaluated, which is made possible by a previously implemented recurrence formula.[55] High rank multipole moments are then required, which are generated by a modified version of MORPHY called MORPHY01.[56] An interaction rank up to $L = 20$ is used for the multipole expansion of the 1−4 interaction energy. To combat divergence in the multipole expansion, we applied the "shift" method, which was originally proposed by our group. Further details are provided in refs 35 and 36. Evidence accumulated in the current work suggests that the shift method does actually work for 1−2 interactions *in principle,* contrary to our previous statement, but the difficulty lies in determining over which distance the original expansion sites need to be shifted to reproduce the six-dimensional "exact" 1−2 interaction energy.

Obtaining smooth energy curves proved very challenging for the CC torsion in acetamide and in the three torsions in *N*-methylacetamide, essentially due to current software limitations. One of the causes is the near-presence of a ring critical point in the $\omega = 180°$ conformation in *N*-methylacetamide (Figure 1a). A ring critical point appears in Figure 1b,d and represents a local maximum in the electron density in one direction (i.e., perpendicular to the ring) and a minimum in two directions (i.e., on the ring plane). The (local) curvature pattern of a ring critical point is therefore (max,min,min), which is opposite to (min,max,max), which is the curvature pattern of a bond critical point. There is duality between these two types of saddle point. One should bear in mind that the rotational energy profiles we are interested in arise from differences between energies often 3 orders of magnitude larger. Jagged curves may appear when energy fluctuations are of the order of 1 kJ mol^{-1} or less. The very short-range interactions (1−2 and 1−3) are potentially most at risk and affect a minority of atom−atom interactions in the larger systems. Only one or two such interactions can spoil the overall sum that we wish to report.

We should clarify which atoms are included when we report $1 - n$ interaction energies below. For a variation in the ABCD dihedral angle, all atoms bonded to atoms B and C, are included in the 1−4 interaction energy. For example, there are $3 \times 3 = 9$ H···H interactions in ethane that count toward a total 1−4 interaction energy. Moreover, if more atoms are bonded to B and C (such as in acetamide, when B and C represent the C−N bond) then the $1 - n$ ($n > 4$) interactions are also added to the 1−4 interaction energies.

3. Results and Discussion

Figure 3 shows a full energy partitioning of five molecules (ethane, peroxide, hydrazine, methanol and formamide) at the HF/6-31G(d) level during relaxed rotation around a central bond. Figure 3a shows the energy changes due to rotation around the central CC bond relative to the staggered energy minimum at 60°. The Hartree−Fock energy barrier for relaxed rotation is found to be 11.5 kJ mol^{-1}. For our purposes this is close enough to the B3LYP/6-311+(2d,p) value of 11.2 kJ mol^{-1} or even to the previously reported[57] value of 12.2 kJ mol^{-1} at MP2/6-311+G(3df,2p) level. The "ab initio" curve and the "total" curve are closely aligned
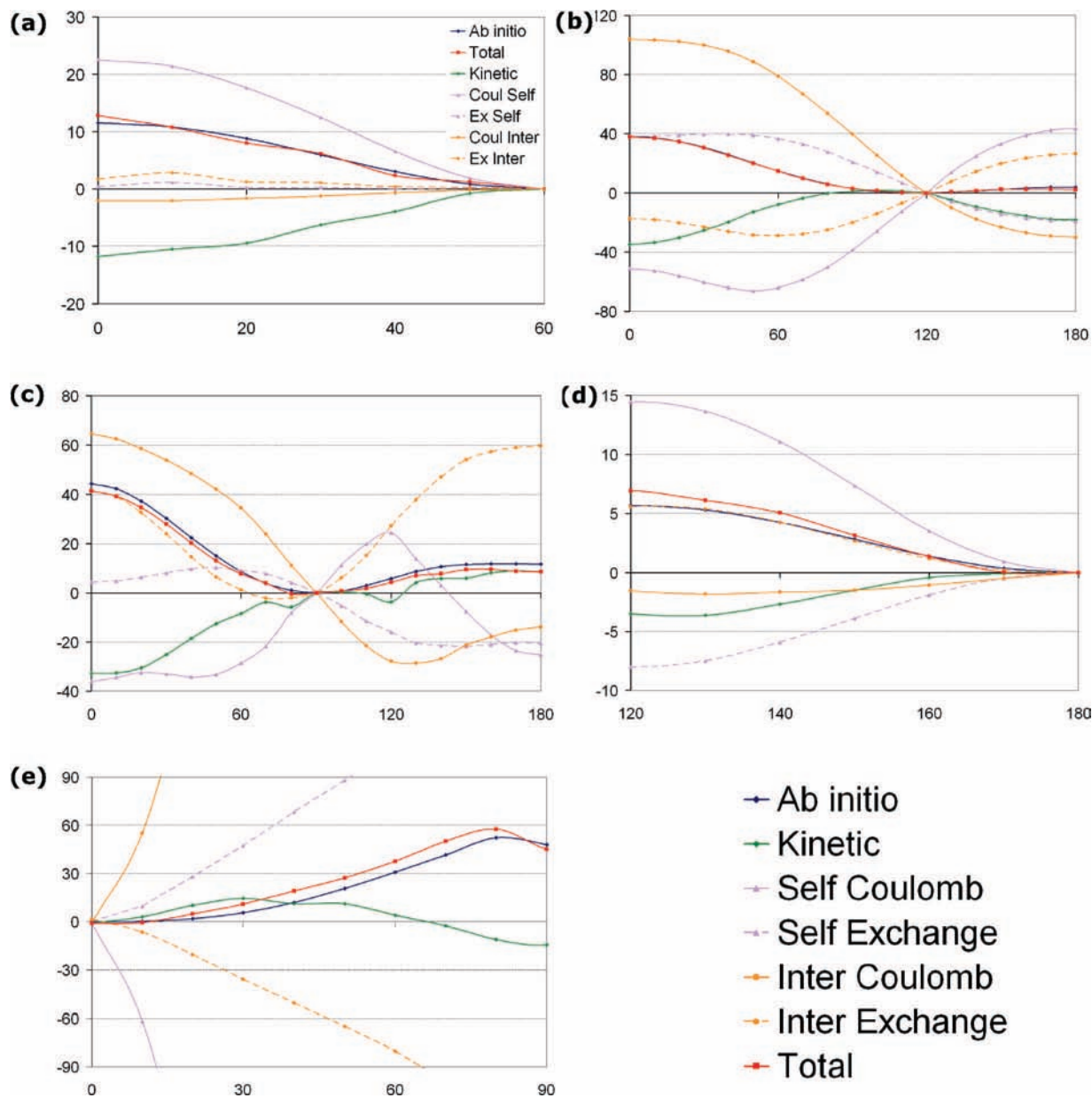
Figure 3. Full energy partitioning of (a) ethane (CC rotation), (b) peroxide (OO rotation), (c) hydrazine (NN rotation), (d) methanol (CO rotation) and (e) formamide (CN rotation). Energies changes (kJ mol^{-1}) due to relaxed rotation around a relevant central bond specified above are shown relative to an energy minimum, where the curves intersect. ("Ab initio" = original unpartitioned Hartree−Fock energy; "Total" is the sum of Self Coulomb, Self Exchange, Inter Coulomb, Inter Exchange and Kinetic).

with deviation of the order of 1 kJ mol^{-1}. This corresponds to a relative error of about 10%, which shows that the partitioning algorithm is adequate for a semiquantitative discussion. Although 10% may seem large, one should bear in mind that this total energy was obtained from much larger numbers that partially cancel each other. The self-energies, for example, are of the order of 10^5 kJ mol^{-1}. The most striking feature of this plot is that the Coulomb self-energy is the dominant contribution to the barrier. Note that all eight atoms contribute to this energy profile. The second most important contribution, the kinetic energy, actually works against the barrier, favoring the eclipsed conformation (0°). Still, it is about half the magnitude of the Coulomb self-energy and is hence not able to cancel the latter contribution. It is tempting to relate this kinetic energy decrease with the observed swelling of atomic volumes while approaching the eclipsed conformation. If, loosely speaking, the electron density in a topological atom can be compared with the

particle-in-a-box system, then this is what the Heisenberg principle would predict. The kinetic energies of the two carbons are almost solely responsible for the total energy profile and are only marginally countered by the contribution from the six hydrogens. Figure 3a shows that the remaining terms, exchange (both self- and interaction) and the Coulomb interaction energy, are about an order of magnitude smaller than the kinetic or Coulomb self-energy terms. An atomic decomposition of the Coulomb interaction term reveals (not shown) that the CC interaction is largely responsible for its profile. The covalent CH interactions actually counter this profile, whereas the noncovalent CH interactions are an order of magnitude weaker and hence hardly exert any influence. Finally, approaching the eclipsed conformation increases the HH interaction between two eclipsing hydrogens to about 0.1 kJ mol^{-1}, which amounts to only 5% of the total Coulomb interaction energy.

Short-Range Electrostatics in Torsional Potentials

J. Phys. Chem. A, Vol. 112, No. 50, 2008 **12959**

Figure 3b confirms an even closer agreement between the "ab initio" curve and the "total" curve with a deviation of 0.3 kJ mol^{-1} at the barrier at 0°. The partitioning of hydrogen peroxide shows a qualitative different picture to ethane. For angles less than 120° the curve dominant in building up the rotation barrier is now the Coulomb interaction energy, which is substantially countered by the Coulomb self-energy. The exchange energies oppose each other as well, with the self-energy aiding the barrier and the interaction energy countering it. For angles larger than 120° this situation is reversed. Curiously, below 120°, the kinetic energy is almost a "negative" mirror image of the total energy, whereas for angles larger than 120° the kinetic energy profile is virtually identical to the self-exchange energy. Clearly, the rotational energy profile of this simple molecule results from a complex interplay of physically well-defined components. Moreover, the qualitative details of this complicated pattern is different to that of another simple molecule, ethane.

The energy decomposition of hydrazine is the most complicated of all molecules studied, as shown in Figure 3c. Here, the deviation between "total" and "ab initio" energy is much larger, about 3 kJ mol^{-1} at the barrier at 0°. Fortunately, this deviation is more than an order of magnitude smaller than the size of the five energy curves for many values of the rotation angle. For angles below 90°, hydrazine shares with hydrogen peroxide the feature that the Coulomb interaction energy dominates the energy buildup toward the rotation barrier at 0°, again predominately countered by the Coulomb self-energy. The kinetic energy again opposes the total energy profile, but only for angles below 90°.

Figure 3d shows the decomposition of methanol's rotation profile, which is broadly similar to that of ethane. Again, the Coulomb self-energy is prevailing. The computational energy discrepancy ("fluctuation") now amounts up to just over 1 kJ mol^{-1} at the barrier at 0°. The main difference with ethane is important role of the exchange self-energy in countering the rotation barrier. The exchange interaction energy is also more pronounced than in ethane, although qualitatively similar.

Figure 3e closes the energy decomposition analysis with the case of formamide rotation around the CN bond. The rather large rotation barrier (52.4 kJ mol^{-1} exact and 57.6 kJ mol^{-1} after reconstruction, i.e., "total") is due to a subtle cancelation of massively opposing contributions. The Coulomb interaction energy aids the barrier but is almost completely countered by the Coulomb self-energy. For the pair of exchange energies the situation is just the opposite: now the self-energy aids the barrier and the interaction energy counters it. The kinetic energy initially helps the barriers to then eventually oppose it from roughly 50° onward.

Figure 4 shows the decomposition of the Coulomb interaction energy in terms of 1−2, 1−3 and 1−4 interactions for rigid rotation around the central CC bond in ethane. As already made clear by Figure 3a, the Coulomb interaction energy fails to reproduce the relaxed rotation barrier, which was found to be 11.2 kJ mol^{-1} (the barrier for rigid rotation is 11.7 kJ mol^{-1}). Instead, the Coulomb interaction energy of the staggered conformation (0°) is almost 2 kJ mol^{-1} *lower* than that of the eclipsed conformation (60°). Only the 1−4 interaction energy gives rise to a rotation barrier, albeit much too small (0.5 kJ mol^{-1}), whereas both the 1−2 and 1−3 interactions decrease in energy toward the eclipsed conformation. The 1−2 interactions can be decomposed further in terms of atom−atom (AB) interactions, which are not shown. In the rigid rotation picture, only the CC energy profile adds to the energy barrier, whereas
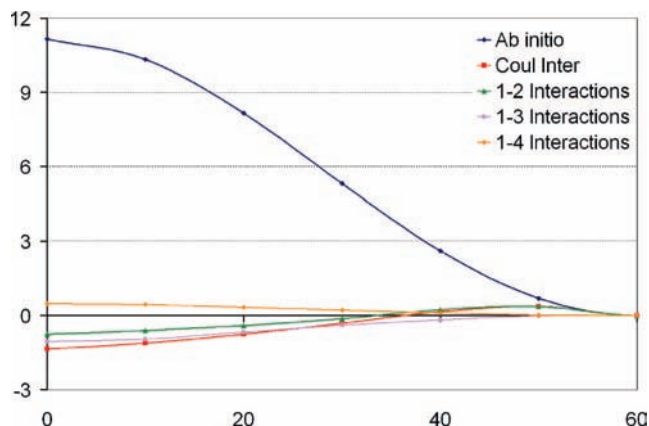

Figure 4. Decomposition of Coulomb interaction energy (kJ mol^{-1}) in terms of 1−2, 1−3 and 1−4 interactions for relaxed rotation (angle in degrees) around the central CC bond in ethane.
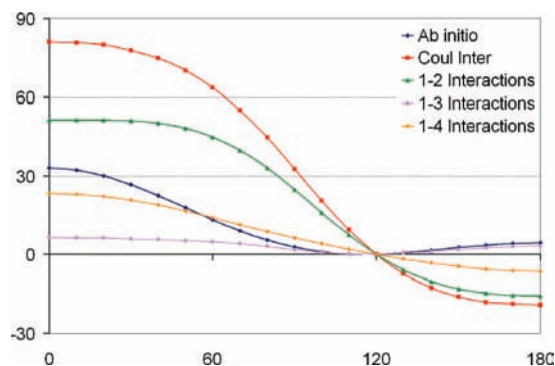

Figure 5. Decomposition of Coulomb interaction energy (kJ mol^{-1}) in terms of 1−2, 1−3 and 1−4 interactions for relaxed rotation (angle in degrees) around the central OO bond in hydrogen peroxide.

the six identical CH interactions counteract it. Because the CH interactions outweigh the CC interaction the overall barrier due to 1−2 interactions disappears. In the relaxed rotation picture, the balance between atom−atom contributions is more complex. Here the CC interaction counteracts the barrier (by 3 kJ mol^{-1} at 0°), in complete contrast to the behavior in the rigid regime. This is largely due to the C−C bond length increases by 0.014 Å in the eclipsed conformation compared to the staggered conformation. This lengthening is seen regardless of the level of theory used.[58] The three CH 1−2 interaction energies summed over each methyl group give identical profiles, with a minimum at 60° (staggered) and a maximum of 1.1 kJ mol^{-1} at 0° (eclipsed).

Figure 5 illustrates the same analysis for hydrogen peroxide as shown in Figure 4 for ethane, but now referring to B3LYP/6-311+G(2d,p) geometries. The relaxed rotation barrier of 33.1 kJ mol^{-1} between the global energy minimum and the *cis* transition state at 0° agrees very well with previous work[57] reporting 32.6 kJ mol^{-1} at MP2/6-311+G(3df,2p) level. This minimum occurred at 115.9° in this work (appearing as 120° in Figure 5) and at 111.9° at MP2 level. For this polar molecule the qualitative picture is very different from that of ethane. In the case of hydrogen peroxide the (total) Coulomb interaction energy aids the rotation barrier and even overshoots it by more than 100%. All types of interactions, that is, 1−2, 1−3 and 1−4, create the desired rotation barrier although 1−3 interactions do so only weakly. Curiously, the 1−3 energy profile almost coincides with the original ab initio energy profile in the interval between the global minimum at the other transition state at 180°.
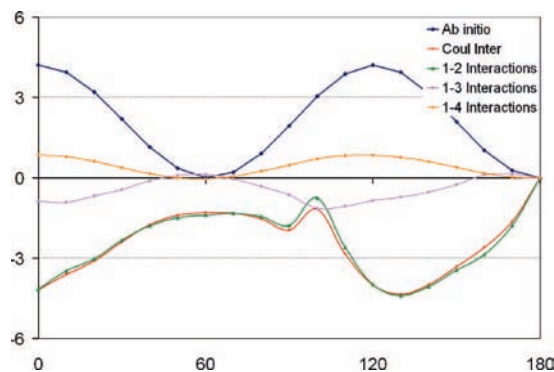
Figure 6. Decomposition of Coulomb interaction energy (kJ mol^{-1}) in terms of 1−2, 1−3 and 1−4 interactions for relaxed rotation (angle in degrees) around the central CO bond in methanol.

Figure 7. Decomposition of Coulomb interaction energy (kJ mol^{-1}) in terms of 1−2, 1−3 and 1−4 interactions for relaxed rotation (angle in degrees) around the central CC bond in acetaldehyde.

A second typical polar molecule for which rotational energy profiles have been studied is hydrazine. Despite its simple structural features, the origin of the rotation barrier has not yet been resolved.[59] When varying the torsion angle around the central NN bond, one finds a global minimum and two transition states, one called *cis* in which the two pairs of hydrogen eclipse each other, and the other called *trans*, where each hydrogen is in an *anti* configuration with respect to the other hydrogen. The rotation barrier over the *cis* conformation is much larger than that over the *trans* conformation. For rigid rotation, the barrier at the B3LYP/6-311+G(2d,p) level is 42.6 kJ mol^{-1} for *cis* and 26.2 kJ mol^{-1} for *trans*. For relaxed rotation the barrier energies are higher at 37.0 and 12.4 kJ mol^{-1}, respectively. For rigid rotation the ground state has a torsion angle of 100° and the relaxed rotation yields a torsion angle of 90°. Song et al.[59] calculated the torsion angle to be 91.2° at the B3LYP/6-31++G** level, and Graña and Mosquera[60] found the angle to vary from 89.7° to 90.1° at four different levels (HF, MP2, QCSID and B3LYP). Chung-Phillips and Jebber reported[57] 37.5 and 13.7 kJ mol^{-1} for the *cis* and *trans* barriers, respectively, at the MP2/6-311+G(3df,2p) level with the global minimum at 90.2°.

Figure S2 (Supporting Information) shows only a very broad agreement between the ab initio energy profile and the Coulomb interaction energy profile. This is only true for the *cis* barrier though. The Coulomb energy yields a rotation barrier of 45.3 kJ mol^{-1} whereas the ab initio barrier is 37.3 kJ mol^{-1} or an overestimation of 8 kJ mol^{-1}. The Coulomb energy minimum is also shifted to 120° whereas the Gaussian minimum is at 90° The Coulomb energy does not show a barrier at all for the *trans* conformer. The 1−4 interactions are about an order of magnitude smaller than the 1−2 or 1−3 interactions and hence play a minor role.

Increasing the number of atoms involved in the torsional barrier from hydrogen peroxide over hydrazine naturally leads to methanol, which features the ubiquitous methyl group now in contact with a lone pair system (OH). The barrier to internal rotation around the CO bond was calculated at the MP2/6-311+G(3df,2p) level to be 4.27 kJ mol^{-1}[57] and 4.16 kJ mol^{-1} at the MP2/aug-cc-pTVZ level.[61] Like ethane, methanol adopts a staggered conformation in the optimized geometry and has an eclipsed conformation at the top of the barrier. However, the rotation barrier is almost 3 times lower for methanol than it is for ethane. The barrier to relaxed rotation calculated here is 4.2 kJ/mol, with minima at 60° and 180° and maxima at 0° and 120°.

Figure 6 demonstrates that the Coulomb interaction energy fails to reproduce the rotation barrier. Instead, like for ethane,
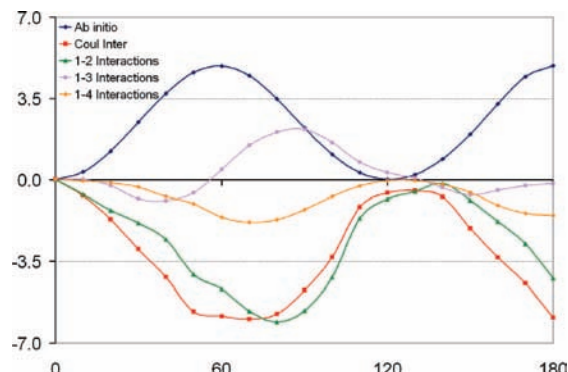
the staggered geometry (180°) turns out higher in energy than the eclipsed geometry (0°). Remarkably, the (total) Coulomb profile closely matches the 1−2 interaction energy, which is dominated by the CO and OH contributions. The fact that the 1−2 profile matches the total profile necessarily means that the 1−3 (7 terms) and 1−4 interactions (3 terms) approximately cancel each other. For the rigid rotation this is not quite true (not shown). Remarkably, the three CH 1−2 interaction energies summed over the methyl group vanish. The CO and OH 1−2 interaction energies oppose each other, where CO promotes the rotation barrier and OH counteracts it, in a predominate manner.

The next most complex molecule that has received considerable experimental and theoretical attention is acetaldehyde.[62] The rotation of the methyl group around the C−C bond was investigated by varying the HCCO torsion angle. This angle is (approximately) 0° in the optimized geometry where one methyl hydrogen is eclipsed with the carbonyl oxygen. The barrier to rigid rotation is 6.4 kJ mol^{-1}, and the barrier to relaxed rotation is 4.9 kJ mol^{-1}. This is slightly higher than the 4.75 kJ mol^{-1} calculated by Xu et al.[63] at the MP2/6-311+G(3df,2p) level.

Figure 7 shows that the ab initio energy profile is not reproduced by the Coulomb interaction energy profile. The latter is almost reproduced by the 1−2 interaction only. This interesting observation is reminiscent of the more dramatic match seen in methanol. The lengthening of the C−C bond has been highlighted as a key factor in the rotation barrier of ethane. The C−C bond of acetaldehyde also lengthens during methyl rotation. In fact, Goodman and co-workers asserted[62] that torsional rotations about X−CH$_3$ bonds lead to X−C bond lengthening in general. The optimized bond length is 1.502 Å, and this increases to 1.510 Å at 60°. The three CH 1−2 interaction energies summed over the methyl group yield a very shallow profile reaching 0.4 kJ mol^{-1} at most, reminiscent of the cancelation found in the case of methanol. Only the C$_{carbonyl}$H 1−2 interaction energy aids the rotation barrier, whereas the single bond CO and CC interactions counteract it.

Internal rotation around the C−N bond in formamide was investigated next. Formamide is a fundamental building block of proteins (and hence enzymes) and is one of the simplest molecules to study the hydration of an amide group with. However, it should be noted that formamide, though considered prototypical for the amide linkage, is not typical.[64] Formamide undergoes internal rotation via two transition states and five of its six atoms can participate in hydrogen bonding. The barrier increases as the polarity of the solvent used increases.[65] Experimental determination of the barrier height is very difficult due to the coupling between internal rotation and nitrogen inversion and was found to be 69.5 kJ mol^{-1}.[66] Forgarasi and

Short-Range Electrostatics in Torsional Potentials

J. Phys. Chem. A, Vol. 112, No. 50, 2008 **12961**

Szalay[67] calculated the barrier to be 63.6 kJ mol^{-1} at CCSD(T)/ PVTZ level. Both rigid and relaxed rotations reach a maximum at 90° and have minima at 0° and 180°. The barrier to rigid rotation is 108.7 kJ mol^{-1} whereas for relaxed rotation it is 53.1 kJ/mol.

Figure S3 (Supporting Information) compares the Coulomb interaction energy profile (and its decomposition) with the ab initio profile. Although the Coulomb profile helps toward the establishment of the ab initio rotation barrier, it dramatically overshoots it. The enormous contribution from the 1−2 interactions is predominantly due to the C−N interaction with the other interactions all working in the same vein. The huge C−N contribution is related to the CN bond lengthening, which is typical during relaxed rotations. During rotation from planar to 90° the length of the C−N bond increases by 0.06 Å, while the C=O bond shortens by 0.01 Å, which is confirmed by experiment.[68] Also the NH$_2$ group, which is planar in the optimized geometry, adopts a pyramidal arrangement with an H−N−H angle of 103.3° at a torsional angle of 90°. The 1−3 interactions work against the rotation barrier, which is largely caused by the O···H$_{carbonyl}$ interaction, followed by the O···N interaction at about half the magnitude. The 1−4 interactions are at least an order of magnitude smaller than the 1−2 or 1−3 interactions, and the sudden energy drop is due to the relaxation effect explained in Figure S1 (Supporting Information). During rigid rotation (not shown) the total Coulomb interaction energy is reduced by about an order of magnitude. We note that during relaxed rotation both the oxygen and nitrogen atoms become less negatively charged, going from planar to 90°, while the carbon becomes less positively charged.

The internal rotation around the C−N bond in acetamide was investigated next. Rotation around this bond is important because it provides information on the conformational preference of protein and peptide backbones.[69] The optimized geometry has a planar NH$_2$ group and a methyl hydrogen lying in the OCN plane (O=C and C−H being staggered). We first discuss the rotation around the CN bond. The presumably[70] partial double-bond character of the C−N bond gives a high barrier to internal rotation[1] of 60−95 kJ mol^{-1}. The HNCO torsion was varied from 0° (the optimized geometry) to 180°. Both rigid and relaxed rotation shows an increase in energy as the NH$_2$ group is rotated from 0° to 90°. The barrier for rigid rotation is 109 kJ mol^{-1}, and the barrier to relaxed rotation is more than 50% lower at 48 kJ mol^{-1}. Acetamide has eight 1−2 interactions, twelve 1−3 interactions and sixteen 1−4 interactions. The energy decomposition of the Coulomb interaction and the ab initio energies for the relaxed NH$_2$ rotation is shown in Figure S4 (Supporting Information). The energy profiles are similar to those of Figure S3 (Supporting Information), hinting at the transferable nature of the O=C−NH$_2$ torsion potential. The 1−2 and 1−4 interactions again dramatically rise in energy as the NH$_2$ group is rotated while the 1−3 interactions becomes more favorable.

As expected, the rotation around the CC bond is much more facile than that around CN. The rotation barrier is only 0.6 kJ mol^{-1} calculated at our level of theory. The three CH 1−2 interaction energies summed over the methyl group yield a profile counteracting the rotation barrier with a minimum of −1.7 kJ mol^{-1}. The CC interaction is approximately in sync with the methyl group with a minimum of about −6.2 kJ mol^{-1}.

The final molecule studied is *N*-methylacetamide. In proteins and peptides the barrier hinders the higher energy *cis* form from relaxing to the more stable *trans* form. The rate of *cis−trans* isomerization is often the rate-determining step of folding and refolding of various proteins.[71] *N*-Methylacetamide contains
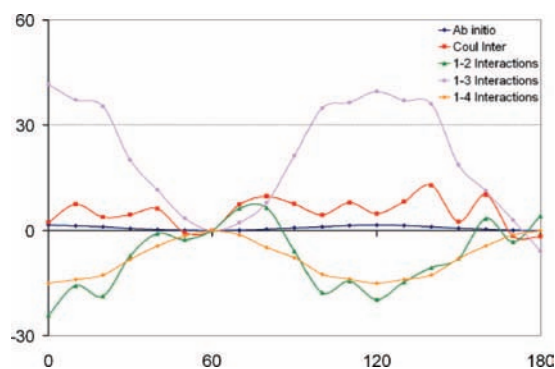

Figure 8. Decomposition of Coulomb interaction energy (kJ mol^{-1}) in terms of 1−2, 1−3 and 1−4 interactions for relaxed rotation (angle in degrees) around the NC$_{methyl}$ bond in *N*-methylacetamide.

three torsion angles of interest: around CC, C$_{carbonyl}$N (i.e., the peptide bond) and CN. In view of the technical difficulties described in section 2.4 we obtained (sufficiently) smooth energy profiles only for the latter two torsion angles, shown in Figure S5 (Supporting Information) and Figure 8, respectively. The molecule was optimized in its *trans* conformation (the peptide torsion angle being defined as 180° here). Figure 8 shows the very shallow ab initio energy barrier at 120° compared to the minimum at 180°. The Coulomb interaction energy roughly follows this barrier, albeit it several factors more exaggerated. Only the 1−3 interactions support the barrier, whereas the 1−2 and 1−4 interactions counter it, in almost equal measure. Compared with the other molecules it is remarkable that the 1−2 interaction does not dominate the total Coulomb interaction. Figure S5 (Supporting Information) is the counterpart of Figure 8 but now for the peptide torsion angle around the central C$_{carbonyl}$N bond. As expected, the ab initio rotation barrier is large (67 kJ mol^{-1}), which is even more dramatically echoed in the Coulomb interaction profile. Again, the 1−2 interaction is responsible for the huge Coulomb barrier, but the 1−3 interactions opposes it quite substantially. In view of the importance of peptide bonds in proteins, and given that *N*-methylacetamide is a prototypical molecule, it is worth disentangling the 1−4 interactions into atom−atom contributions. Figure S6 (Supporting Information) shows the most important atom−atom interactions as the central peptide torsion angle varies from 180° to 160°. The H11 atom, which almost participates in a five-membered intramolecular hydrogen bonded ring, is prominent. The O···H11 interaction becomes less stable upon torsional rotation (i.e., away from 180°), almost equally opposed by the C$_{carbonyl}$···H11 interaction. Three more dominant but much smaller interactions are shown, and all other remaining 1 − n (n ≥ 4) interactions are even smaller. We point out that the peptide torsion analysis was carried out using the OCNH torsion angle as a control variable. Choosing the CCNC torsion angle reduces the rotation barrier to 58 kJ mol^{-1} and shifts it from near 80° to 100°.

The CH 1−2 interaction energies summed for each methyl group (not shown) separately yield a profile for the rotation around CC and for the rotation around CN. Curiously, the methyl energy profile of the latter almost matches the ab initio energy profile. The CC methyl profile, however, is almost a perfect mirror image, countering the ab initio profile.

After a detailed inspection of the energetic behavior of atom−atom Coulomb interactions during rotation, it is helpful to survey all energy profiles. Figure 9 presents, in a single tableau, the difference between the ab initio and Coulomb interaction energy profiles, for both rigid and relaxed rotation.
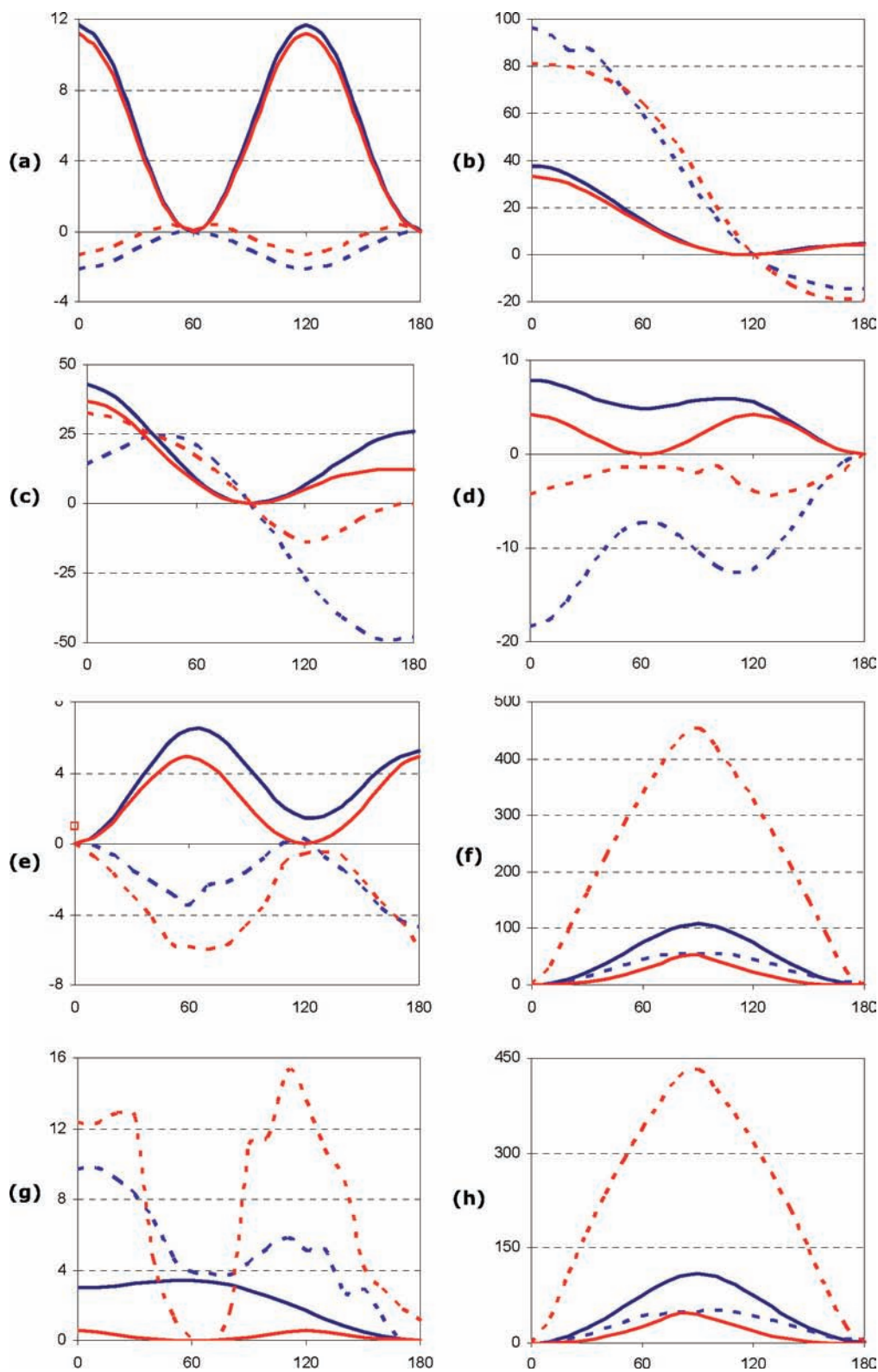
Figure 9. Ab initio (solid) and Coulomb interaction (dashed) energy profiles for rigid (blue) and relaxed (red) rotation as each of the eight torsion angles in a set of seven molecules is varied (see Figure 2). The torsion angle is varied in 10° steps between 0° and 180°. At each point, only the torsion angle is fixed; all other internal coordinates are allowed to relax. The relative energy (kJ mol^{-1}) is shown on the left-hand *y*-axis, and the angle is along the *x*-axis. Key: (a) ethane C−C rotation, (b) hydrogen peroxide O−O rotation, (c) hydrazine N−N rotation, (d) methanol C−O rotation, (e) acetaldehyde C−C rotation, (f) formamide C−N rotation, (g) acetamide C−C rotation and (h) acetamide C−N rotation.

In none of the eight torsional energy profiles do the Coulomb and ab initio profiles match. This is so for both the rigid and relaxed rotation. Hence, torsion profiles are not of an electrostatic nature, in terms of atom−atom interactions. At

best, the Coulomb interaction aids the rotation barrier, which is only true for the peptide bond rotations (formamide and acetamide), the *cis* barriers in hydrogen peroxide and hydrazine. In the other cases, the profiles of the Coulomb
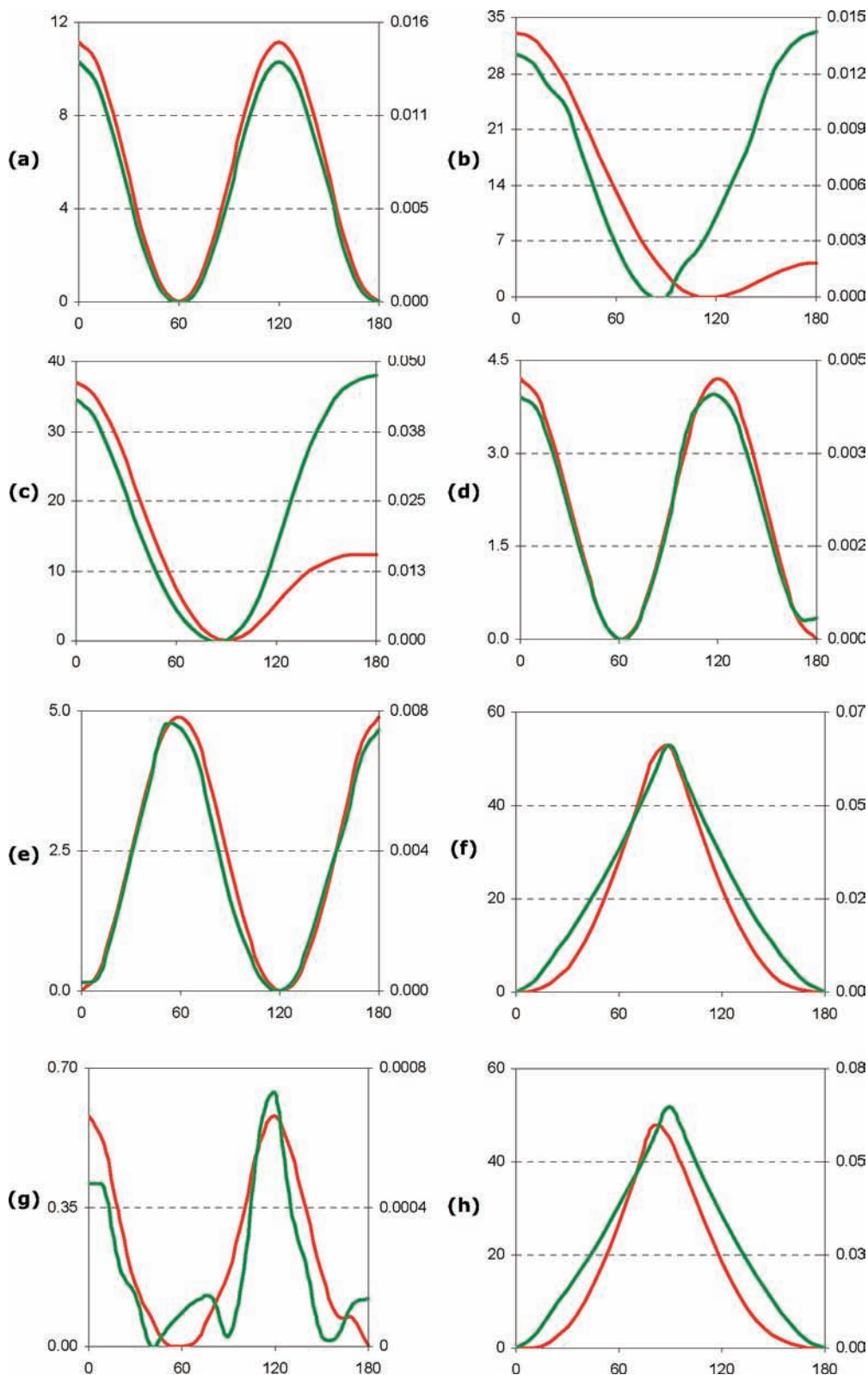
Short-Range Electrostatics in Torsional Potentials

J. Phys. Chem. A, Vol. 112, No. 50, 2008 **12963**

Figure 10. Ab initio rotation energy profiles (red) and bond length variation (green) as each of the eight torsion angles in a set of seven molecules is varied (see Figure 2). The torsion angle is varied in 10° steps between 0° and 180°. At each point only the torsion angle is fixed while all other internal coordinates are allowed to relax. The relative energy (kJ mol^{-1}) is shown on the left-hand y-axis, and the change in bond length (Å) is on the right-hand y-axis; the angle is along the x-axis. Key: (a) ethane C−C rotation, (b) hydrogen peroxide O−O rotation, (c) hydrazine N−N rotation, (d) methanol C−O rotation, (e) acetaldehyde C−C rotation, (f) formamide C−N rotation, (g) acetamide C−C rotation and (h) acetamide C−N rotation.

interaction energy counteract the ab initio one, almost in a mirroring way.

In another tableau covering the same test cases, Figure 10 connects the behavior of an ab initio torsional energy profile

(for relaxed rotation) and the variation in bond length of the central bond in the torsion angle. For ethane (Figure 10a) the bond length increase toward the rotation barrier and faithfully follows the energy profile. This match occurs in spite of other

geometric changes that take place during this relaxed rotation. In hydrogen peroxide (Figure 10b) the increase in OO bond length is roughly the same toward the *cis* barrier as toward the *trans* barrier, in spite of the large difference in rotation barrier. This is also true for hydrazine (Figure 10c). In methanol (Figure 10d) and acetaldehyde (Figure 10e) the curves again tally. This is also the case for rotations around the peptide bonds in formamide (Figure 10), acetamide (Figure 10h) and *N*-methyl-lacetamide (not shown). However, the rotation around CC in acetamide shows less concurrent behavior. The overall values of the curves in Figure 10 demonstrate that a simple but not necessarily causal relationship exists between the variation in the central bond length and the concomitant torsional energy profile.

At the end of this section it is appropriate to summarize overall trends. First, ab initio rotation barriers are already well reproduced by the current medium level of theory compared to more expensive levels, except for rotation around a peptide bond. Second, the absolute value of the (total) $1-2$ interaction energy is always larger than the (total) $1-3$ interaction energy, which is always larger than the (total) $1-4$ interaction energy. The $1-2$ interaction energy can be up to 10 times greater than the $1-3$ and $1-4$ energy. The $1-2$ energies range from 55 kJ mol^{-1} (C$-$C in ethane) to approximately -2300 kJ mol^{-1} (C$=$O in formamide). The $1-2$ energy of the CC bond is the lowest found in this study and is always lower than the CH $1-2$ energy, which ranges from typically 85 to 108 kJ mol^{-1}. The CC and CH $1-2$ interactions are the only ones that have a positive energy; all others have a negative energy. When ordering the $1-2$ energies from the most negative to the most positive value, one recovers the following sequence: C$_{carbonyl}$O > C$_{carbonyl}$N > CO$_{hydroxy}$ > OH > O$_{peroxide}$H > C$_{methyl}$N > NH > CC > CH > OO > NN. This sequence reflects the polarity of the bonds.

4. Discussion and Conclusion

This work does not aim to explain the origin of rotation barriers. To understand what it aims to do, it is useful to reiterate the context of this paper. The long-term goal is to set up a reliable biomolecular force field based on electron density fragments taken from increasingly accurate ab initio wave functions. If we accept that the ultimate description of a protein is a high-quality wave function, then eq 1 will govern[72] its energy decomposition, both in energy type (kinetic, Coulomb and exchange) and in atomic partitioning. That the latter is accomplished through quantum chemical topology is a choice. The important point is that the real physical information of how atoms interact is lurking in reduced density matrices (or the wave function). The central idea behind classical force field design is to project the potential energy surface of a complete molecule onto predetermined relationships between atoms. Take as an example ethane, which is rotated around its central CC bond while its bond lengths and angles are kept constant. An oscillating energy profile will arise, caused by variations in *all* energy contributions in *all* atoms. Yet, the classical force field may assign the energy profile of the whole molecule to nine individual torsional terms, introducing the typical Fourier expansion. Although such formulas may well capture the molecule's energy variation as a result of this type of rotation, one should not forget that it is a mere mapping or a "projection". Even in diatomic molecules there are complex changes in the various quantum mechanical energy contributions in response to a simple bond stretch. Yet, all these changes can be captured by a simple quadratic near the equilibrium geometry, or a Morse potential, over large stretches. Imposing such simple local

relationships onto larger molecules is fraught with hazard. This is probably why torsional parameters keep being adjusted[73] in force fields such as ff94, ff96 and ff99, which are part of the popular AMBER simulation package. Protein backbone dihedral parametrization can be as drastic[74] as simply zeroing the torsion potential for φ and Ψ. Reviews and even textbooks state that the rotational barrier has contributions from both nonbonded interactions (van der Waals and electrostatic) and the "torsional energy". This entanglement means that torsional parameters are intimately coupled to the nonbonded parameters. To help clarify the situation, we decouple, in this paper, the electrostatic contribution from the rest of the interactions. The electrostatics are not monitored by fitted point charges but by real electron density fragments, represented by high-rank multipole moments. The Coulomb interaction energies between atoms are exact, except for the error introduced by current algorithmic and numerical limitations. If the energy profile of $1-4$ interactions counteracts the molecule's rotation barrier, for example, then that result is genuine. Such observations fix lingering questions, recurrently addressed, as to which contributions causes which energy effect. Returning to ethane, the rotational barrier can be reproduced solely by a HCCH torsional energy term, solely by a HH van der Waals repulsion or solely by a HH electrostatic repulsion, as pointed out by Jensen.[75] He continues highlighting that *"... different force fields will have different balances of these terms, and while one force field may contribute a conformational difference primarily to steric interactions, another may have the major determining factor to be the torsional energy, and a third may 'reveal' that it is all due to electrostatic interactions."* This and future work that will look at full energy partitioning (beyond just Coulomb) strives to settle ambiguities such as those quoted above. Of course, the current Hartree$-$Fock energy decomposition analysis is still far off providing any practical or reliable values for correct protein folding in the way that recent AMBER parametrizations attempt, by directly fitting to realistic conformational energy differences.

Supporting Information Available: Figure S1 shows an example of the effect of relaxing the nuclear skeleton upon torsional rotation in acetamide, which leads to a sudden energy drop. Figures S2$-$S5 show the decomposition of Coulomb interaction energy, in terms of $1-2$, $1-3$ and $1-4$ interactions, for relaxed rotation in hydrazine, formamide, acetamide and *N*-methylacetamide (central torsion angle), respectively (analogous to Figure 5). Figure S6 shows the Coulomb interaction energies in *N*-methylacetamide. This information is available free of charge via the Internet at http://pubs.acs.org.

References and Notes

(1) Kawashima, Y.; Usami, T.; Ohashi, N.; Suenram, R. D.; Hougen, J. T.; Hirota, E. *Acc. Chem. Res.* **2006**, *39*, 216.

(2) Popelier, P. L. A.; Lenstra, A. T. H.; Van Alsenoy, C.; Geise, H. *Struct. Chem.* **1991**, *2*, 3.

(3) Kemp, J. D.; Pitzer, K. S. *J. Chem. Phys.* **1936**, *4*, 749.

(4) Leach, A. R. *Molecular Modelling. Principles and Applications*; Addison Wesley Longman: Harlow, Great Britain, 1996.

(5) Sorin, E. J.; Pande, V. S. *J. Comput. Chem.* **2005**, *26*, 682.

(6) Yoda, T.; Sugita, Y.; Okamoto, Y. *Chem. Phys.* **2004**, *307*, 269.

(7) Sorin, E. J.; Pande, V. S. *Biophys. J.* **2005**, *88*, 2472.

(8) Goodman, L.; Pophristic, V.; Weinhold, F. *Acc. Chem. Res.* **1999**, *32*, 983.

(9) Weinhold, F. *Nature* **2001**, *411*, 539.

Short-Range Electrostatics in Torsional Potentials

J. Phys. Chem. A, Vol. 112, No. 50, 2008 **12965**

(10) Pophristic, V.; Goodman, L. *Nature* **2001**, *411*, 565.

(11) Bickelhaupt, F. M.; Baerends, E. J. *Angew. Chem.-Int. Ed.* **2003**, *42*, 4183.

(12) Song, L. C.; Lin, Y.; Wu, W.; Zhang, Q. N.; Mo, Y. R. *J. Phys. Chem. A* **2005**, *109*, 2310.

(13) Cortes-Guzman, F.; Bader, R. F. W. *Coord. Chem. Rev.* **2005**, *249*, 633.

(14) Mo, Y.; Gao, J. *Acc. Chem. Res.* **2007**, *40*, 113.

(15) Bader, R. *Atoms in Molecules. A Quantum Theory*; Oxford Univ. Press: Oxford, GB, 1990.

(16) Popelier, P. L. A. *Atoms in Molecules. An Introduction*; Pearson: London, GB, 2000.

(17) Rafat, M.; Popelier, P. L. A. *J. Comput. Chem.* **2007**, *28*, 292.

(18) Blanco, M. A.; Pendas, A. M.; Francisco, E. *J. Chem. Theor. Comput.* **2005**, *1*, 1096, and references therein.

(19) Pendas, A. M.; Francisco, E.; Blanco, M. A. *J. Phys. Chem. A* **2006**, *110*, 12864.

(20) Francisco, E.; Pendas, A. M.; Blanco, M. A. *J. Chem. Theor. Comput.* **2006**, *2*, 90.

(21) Dudek, M. J.; Ponder, J. W. *J. Comput. Chem.* **1995**, *16*, 791.

(22) Stone, A. J. *Chem. Phys. Lett.* **1981**, *83*, 233.

(23) Kosov, D. S.; Popelier, P. L. A. *J. Phys. Chem. A* **2000**, *104*, 7339.

(24) Popelier, P. L. A.; Joubert, L.; Kosov, D. S. *J. Phys. Chem. A* **2001**, *105*, 8254.

(25) Popelier, P. L. A.; Kosov, D. S. *J. Chem. Phys.* **2001**, *114*, 6539.

(26) Popelier, P. L. A.; Rafat, M. *Chem. Phys. Lett.* **2003**, *376*, 148.

(27) Rafat, M.; Popelier, P. L. A. *J. Chem. Phys.* **2005**, *123*, 204103.

(28) Rafat, M.; Popelier, P. L. A. Topological atom-atom partitioning of molecular exchange energy and its multipolar convergence. In *Quantum Theory of Atoms in Molecules*; Matta, C. F., Boyd, R., Eds.; Wiley-VCH: Weinheim, Germany, 2007; Vol. 5, p 121.

(29) Joubert, L.; Popelier, P. L. A. *Phys. Chem. Chem. Phys.* **2002**, *4*, 4353.

(30) Shaik, M. S.; Devereux, M.; Popelier, P. L. A. *Mol. Phys.* **2008**, xx.

(31) Liem, S.; Popelier, P. L. A. *J. Chem. Phys.* **2003**, *119*, 4560.

(32) Liem, S.; Popelier, P. L. A.; Leslie, M. *Int. J. Quantum Chem.* **2004**, *99*, 685.

(33) Liem, S. Y.; Popelier, P. L. A. *J. Chem. Theory Comput.* **2008**, *3*, 353.

(34) Rafat, M.; Popelier, P. L. A. *J. Comput. Chem.* **2007**, *28*, 832.

(35) Joubert, L.; Popelier, P. L. A. *Mol. Phys.* **2002**, *100*, 3357.

(36) Rafat, M.; Popelier, P. L. A. *J. Chem. Phys.* **2006**, *124*, 144102.

(37) Popelier, P. L. A.; Stone, A. J.; Wales, D. J. *Faraday Discuss.* **1994**, *97*, 243.

(38) Price, S. L. Toward more accurate model intermolecular potentials for organic molecules. In *Rev.in Comp.Chem.*; Lipkowitz, K. B., Boyd, D. B., Eds.; Wiley: New York, 2000; Vol. 14, p 225.

(39) Sagui, C.; Pedersen, L. G.; Darden, T. A. *J. Chem. Phys.* **2004**, *120*, 73.

(40) Brodersen, S.; Wilke, S.; Leusen, F.; Engel, G. *Phys. Chem. Chem. Phys.* **2003**, *5*, 4923.

(41) Day, G. M.; Price, S. L.; Leslie, M. *J. Phys. Chem. B* **2003**, *107*, 10919.

(42) Karamertzanis, P.; Pantelides, C. C. *Mol. Simul.* **2004**, *30*, 413.

(43) Batista, E. R. *J. Chem. Phys.* **2000**, *112*, 3285.

(44) Ponder, J. W.; Case, D. A. *Adv. Protein Chem.* **2003**, *66*, 27.

(45) Qian, W.; Krimm, S. *J. Phys. Chem. A* **2005**, *109*, 5608.

(46) Mooij, W. T. M.; Leusen, F. J. J. *Phys. Chem. Chem. Phys.* **2001**, *3*, 5063.

(47) Sokalski, W. A.; Keller, D. A.; Ornstein, R. L.; Rein, R. *J. Comput. Chem.* **1993**, *14*, 970.

(48) Rafat, M.; Popelier, P. L. A. *J. Comput. Chem.* **2007**, *28*, 2602.

(49) Frisch, M. J.; Trucks, G. W.; Schlegel, H. B.; Scuseria, G. E.; Robb, M. A.; Cheeseman, J. R.; Montgomery, J. A. J.; Vreven, J., T.; Kudin, K. N.; Burant, J. C.; Millam, J. M.; Iyengar, S. S.; Tomasi, J.; Barone, V.; Mennucci, B.; Cossi, M.; Scalmani, G.; Rega, N.; Petersson, G. A.; Nakatsuji, H.; Hada, M.; Ehara, M.; Toyota, K.; Fukuda, R.; Hasegawa, J.; Ishida, M.; Nakajima, T.; Honda, Y.; Kitao, O.; Nakai, H.; Klene, M.; Li, X.; Knox, J. E.; Hratchian, H. P.; Cross, J. B.; Adamo, C.; Jaramillo, J.; Gomperts, R.; Stratmann, R. E.; Yazyev, O.; Austin, A. J.; Cammi, R.; Pomelli, C.; Ochterski, J. W.; Ayala, P. Y.; Morokuma, K.; Voth, G. A.; Salvador, P.; Dannenberg, J. J.; Zakrzewski, V. G.; Dapprich, S.; Daniels, A. D.; Strain, M. C.; Farkas, O.; Malick, D. K.; Rabuck, A. D.; Raghavachari, K.; Foresman, J. B.; Ortiz, J. V.; Cui, Q.; Baboul, A. G.; Clifford, S.; Cioslowski, J.; Stefanov, B. B.; Liu, G.; Liashenko, A.; Piskorz, P.; Komaromi, I.; Martin, R. L.; Fox, D. J.; Keith, T.; Al-Laham, M. A.; Peng, C. Y.; Nanayakkara, A.; Challacombe, M.; Gill, P. M. W.; Johnson, B.; Chen, W.; Wong, M. W.; Gonzalez, C.; Pople, J. A. *GAUSSIAN03*; Gaussian, Inc.: Pittsburgh, PA, 2003.

(50) Goodman, L.; Pophristic, V.; Weinhold, F. *Acc. Chem. Res.* **1999**, *32*, 983.

(51) Goodman, L.; Kundu, T.; Leszczynski, J. *J. Phys. Chem.* **1996**, *100*, 2770.

(52) Popelier, P. L. A. *Mol. Phys.* **1996**, *87*, 1169.

(53) Popelier, P. L. A. *Comput. Phys. Commun.* **1998**, *108*, 180.

(54) Brink, D. M.; Satchler, G. R. *Angular Momentum*, 3rd ed.; Clarendon: Oxford, GB, 1993.

(55) Haettig, C. *Chem. Phys. Lett.* **1996**, *260*, 341.

(56) Popelier, P. L. A.; Bone, R. G. A.; Kosov, D. S. *MORPHY01*; UMIST: Manchester, England, 2001.

(57) Chung-Phillips, A.; Jebber, K. A. *J. Chem. Phys.* **1995**, *102*, 7080.

(58) Goodman, L.; Gu, H. B. *J. Chem. Phys.* **1998**, *109*, 72.

(59) Song, J. W.; Lee, H. J.; Choi, Y. S.; Yoon, C. J. *J. Phys. Chem. A* **2006**, *110*, 2065.

(60) Grana, A. M.; Mosquera, R. A. *J. Mol. Struct.* **2000**, *556*, 69.

(61) Munoz-Caro, C.; Nino, A.; Senent, M. L. *Chem. Phys. Lett.* **1997**, *273*, 135.

(62) Ozkabak, A. G.; Goodman, L. *J. Chem. Phys.* **1992**, *96*, 5958.

(63) Xu, L. H.; Lees, R. M.; Hougen, J. T. *J. Chem. Phys.* **1999**, *110*, 3835.

(64) Demaison, J.; Csaszar, A. G.; Kleiner, I.; Møllendal, H. *J. Phys. Chem.* **2007**, *111*, 2574.

(65) Taha, A. N.; True, N. S. *J. Phys. Chem. A* **2000**, *104*, 2985.

(66) Taha, A. N.; Crawford, S. M. N.; True, N. S. *J. Am. Chem. Soc.* **1998**, *120*, 1934.

(67) Fogarasi, G.; Szalay, P. G. *J. Phys. Chem. A* **1997**, *101*, 1400.

(68) Wiberg, K. B. *Acc. Chem. Res.* **1999**, *32*, 922.

(69) Kang, Y. K.; Park, H. S. *J. Mol. Struct.-THEOCHEM* **2004**, *676*, 171.

(70) Milner-White, E. J. *Protein Sci.* **1997**, *6*, 2477.

(71) Fischer, G. *Chem. Soc. Rev.* **2000**, *29*, 119.

(72) Equation 1 is only valid for restricted Hartree−Fock wave functions but can be replaced by a more general equation valid for an arbitrarily accurate wave function. It then involves reduced density matrices of order 1 and 2, as shown in the "master equation" (2.3.27) in: Parr, P. R.; Yang, W. *DFT of Atoms and Molecules*; Oxford, GB, 1989.

(73) Hornak, V.; Abel, R.; Okur, A.; Strockbine, B.; Roitberg, A.; Simmerling, C. *Proteins: Struct., Funct. Bioinformatics* **2006**, *65*, 712.

(74) Garcia, A. E.; Sanbonmatsu, K. Y. *Proc. Natl. Acad. Sci. U.S.A.* **2002**, *99*, 2782–2787.

(75) Jensen, F. *Introduction to Computational Chemistry*; Wiley: Chichester, England, 1999.